Response of GOLD Retrieved Thermospheric Temperatures to Geomagnetic Activities of Varying Magnitudes

Fazlul I Laskar[1], Richard W Eastes[2], Mihail V. Codrescu[3], Joseph S. Evans[4], Alan G. Burns[5], Wenbin Wang[6], William E. McClintock[2], and Xuguang Cai[7]

[1]Laboratory for Atmospheric and Space Physics, University of Colorado, Boulder, CO, USA
[2]Laboratory for Atmospheric and Space Physics
[3]NOAA-Space Weather Prediction Center
[4]Computational Physics, Incorporated
[5]National Center for Atmospheric Research (UCAR)
[6]HAO/NCAR
[7]HAO NCAR

November 22, 2022

Abstract

Global-scale Observations of Limb and Disk (GOLD) disk measurements of far ultraviolet molecular nitrogen band emissions are used to retrieve temperatures (T_{disk}), which are representative of lower thermospheric altitudes. The present investigation studies the response of lower thermospheric temperatures to geomagnetic activities of varying magnitudes. In this study, it has been observed that T_{disk} increases over all latitudes in response to enhanced geomagnetic activity. The increase in temperature is proportional to the strength of the geomagnetic activity and is greater at higher latitudes. Temperature enhancements vary from 10s to 100s of Kelvins from low- to mid-latitudes. Local time behavior shows that pre-noon enhancements in temperatures, during relatively stronger geomagnetic activities, are greater compared to afternoon, which can be attributed to the combined action of daytime dynamics and geomagnetic forcing. This study thus demonstrates the utility of GOLD T_{disk} measurements investigating the effects of dynamical and external forcings in the thermosphere.

Response of GOLD Retrieved Thermospheric Temperatures to Geomagnetic Activities of Varying Magnitudes

F. I. Laskar[1], R. W. Eastes[1], M. V. Codrescu[2], J. S. Evans[3], A. G. Burns[4], W. Wang[4], W. E. McClintock[1], X. Cai[4]

[1]Laboratory for Atmospheric and Space Physics, University of Colorado, Boulder, CO, USA

[2]Space Weather Prediction Center, NOAA, Boulder, CO, USA

[3]Computational Physics, Inc., Springfield, Virginia, USA

[4]High Altitude Observatory, National Center for Atmospheric Research, Boulder, CO, USA

Key Points:

- GOLD thermospheric temperature increases globally in response to geomagnetic activity
- The increase in temperature is proportional to the strength of the activity and is greater at higher latitudes
- Temperature enhancement during active geomagnetic events is greater in the morning than that in the afternoon.

Corresponding author: Fazlul I. Laskar, `Fazlul.Laskar@colorado.edu`

Abstract

Global-scale Observations of Limb and Disk (GOLD) disk measurements of far ultraviolet molecular nitrogen band emissions are used to retrieve temperatures (T_{disk}), which are representative of lower thermospheric altitudes. The present investigation studies the response of lower thermospheric temperatures to geomagnetic activities of varying magnitudes. In this study, it has been observed that T_{disk} increases over all latitudes in response to enhanced geomagnetic activity. The increase in temperature is proportional to the strength of the geomagnetic activity and is greater at higher latitudes. Temperature enhancements vary from 10s to 100s of Kelvins from low- to mid-latitudes. Local time behavior shows that pre-noon enhancements in temperatures, during relatively stronger geomagnetic activities, are greater compared to afternoon, which can be attributed to the combined action of daytime dynamics and geomagnetic forcing. This study thus demonstrates the utility of GOLD T_{disk} measurements investigating the effects of dynamical and external forcings in the thermosphere.

Plain Language Summary

The thermosphere ionosphere system is influenced by waves from the lower atmosphere and solar and geomagnetic forcing from above. For such a coupled system it is important to decipher the relative influence of the two regimes of forcings. The recently launched GOLD mission provides daytime thermospheric temperatures with unprecedented local time and spatial coverage. The thermospheric temperature over the Earth's disk visible from geostationary orbit is a first of its kind of measurement, which enables us to investigate the local time behavior over wide latitudinal coverage from 69°S to 69°N. We find that, during active geomagnetic conditions, the thermospheric temperature is enhanced across the whole visible hemisphere, with the largest temperature enhancements at higher mid-latitudes. The local time behavior shows that the pre-noon enhancement in temperature is greater compared to the afternoon, which demonstrates, for the first time, the interplay between thermospheric weather and geomagnetic forcing effects.

1 Introduction

Temperature variability of the daytime thermosphere of the Earth is controlled mainly by solar radiation. It is also influenced by wave forcing from the lower atmosphere and geomagnetic forcing from above. During geomagnetic storms energetic particles precip-

itate into the atmosphere at high-latitudes, which induces, among other effects, ionospheric current systems, Joule heating, and circulation changes (Rishbeth & Garriott, 1969; Mayr et al., 1978; Prölss, 1980; Burns & Killeen, 1992; Deng et al., 1995; Forbes et al., 1996; Killeen et al., 1997). The impact of the currents generated by the movement of the energetic particles and the ionization they produce is instantaneous and they can indirectly alter the low-latitude ionosphere (Tsurutani et al., 2008). The most important heating term is the Joule heating (per particle) and the ion-neutral momentum coupling induced by circulation changes give rise to delayed impact at different latitudes and altitudes in the thermosphere (Mayr et al., 1978; Prölss, 1980; Burns et al., 1995).

Depending on the strength of a geomagnetic storm, the thermospheric circulation can reverse from the usual poleward daytime circulation. Storm induced circulation changes can also give rise to relative adiabatic cooling or heating depending on the relative changes in the divergence and convergence of the horizontal winds. Radiative cooling by infrared emissions from nitric oxide (NO) and carbon dioxide (CO_2) is the mechanism through which energy is dissipated in the lower thermosphere (Killeen et al., 1997; Mikhailov & Perrone, 2020). In short, a geomagnetic storm can alter the whole thermosphere-ionosphere (TI) system enormously, so synoptic observations of local time variability of the thermosphere during storm events is important for a complete understanding of space weather.

The neutral atmosphere at TI altitudes (about 100 km and up) is primarily investigated using in-situ (e.g. Spencer et al., 1981; Forbes et al., 1996; H. Liu & Lühr, 2005) and optical remote sensing techniques (Pant & Sridharan, 1998; Pallamraju et al., 2004; Aksnes et al., 2006; Pallamraju et al., 2013; Meier et al., 2015). The temperature of the thermosphere can be retrieved from spectral broadening characteristics of atomic lines (Biondi & Meriwether, 1985; Fagundes et al., 1996; Pant & Sridharan, 1998; Chakrabarty et al., 2002) or molecular bands (Aksnes et al., 2006; Meier et al., 2015; Evans et al., 2018; Zhang et al., 2019). Ground based observations of the thermosphere have good local time coverage, at a cadence of minutes to hours for over at least 10 hours per day, but they are mostly limited to the night-time sector and are available from limited ground stations (Biondi & Meriwether, 1985; Fagundes et al., 1996; Pant & Sridharan, 2001; Chakrabarty et al., 2002). Satellite based remote-sensing observations on the other hand have poor local time coverage and are mostly from limb viewing geometry (Aksnes et al., 2006; Meier et al., 2015). In-situ temperature measurements are also very limited, for example those from Dynamic Explorer 2 (DE-2) mission (Spencer et al., 1981) or those retrieved from

satellite drag (e.g., Mehta et al., 2017, and references therein). The in-situ satellite based measurements also lack local time coverage. Thus, the earlier studies provided mostly a seasonally averaged or near-single local time behavior of the thermospheric temperature variability during geomagnetic activities. Thus, the local time variations of the geomagnetic storm effects on thermospheric temperatures with global coverage have been limited mainly to model simulations only (Burns et al., 1995). For wide spatial and local time coverage one would require ground based stations covering the globe, or a constellation of sun-synchronous satellites in low-earth-orbit, or measurements from the geostationary orbit. The Global-scale Observations of the Limb and Disk (GOLD) mission, launched on 14 January 2018, is in geostationary orbit and provides Far-Ultraviolet (FUV) emission measurements, which can be used to retrieve thermospheric neutral temperatures (Eastes et al., 2020). Though GOLD disk measurements are limited over a fixed hemisphere, they have very good coverage in latitude (69°S to 69°N), longitude (25°E to 120°W; covering America and parts of Europe and Africa), and local time (a minimum of 6 to 18 hr near nadir longitude, which extends to even more depending on location).

Evidence of geomagnetic storm related changes in thermospheric temperatures, densities, and winds are ample in the literature (Mayr et al., 1978; Burns & Killeen, 1992; Burns et al., 1995; Strickland et al., 1999; Pant & Sridharan, 2001; Pallamraju et al., 2004; Crowley et al., 2006; Aksnes et al., 2007; Bagiya et al., 2014; Astafyeva et al., 2020; Karan & Pallamraju, 2018; Zhang et al., 2019; Mandal & Pallamraju, 2020). Due to particle precipitation, the temperatures at high-latitude are increased and the resulting circulation changes alter the whole thermospheric temperature (Burns & Killeen, 1992; Fuller-Rowell et al., 1994; Burns et al., 1995) with some delayed response at different altitudes and latitudes (Burns et al., 1995; X. Liu et al., 2018; Li et al., 2018). Some recent investigations using GOLD O/N_2 (ratio of atomic oxygen and molecular nitrogen column densities) and limb temperature data showed that even minor to moderate geomagnetic activities can impact the TI system significantly (Cai et al., 2020; Evans et al., 2020). But these earlier investigations of daytime thermospheric variability lack the local time and spatial coverage provided by the GOLD mission from geosynchronous orbit. The current study aims to use GOLD disk temperature (T_{disk}) data to investigate synoptic and local time behavior of the thermospheric temperature during periods of enhanced geomagnetic activity of varying magnitudes.

2 Data and Methods

The primary dataset used in this investigation is the GOLD retrieved disk temperatures, T_{disk}. Solar and geomagnetic indices are also used. GOLD observes the Earth's thermosphere in the FUV for over 18.5 hours each day, from 0610 to 0040 UT of the next day (Eastes et al., 2019, 2020; McClintock et al., 2020; Laskar et al., 2020; Cai et al., 2021). GOLD daytime disk scans of the N_2 Lyman-Birge-Hopfield (LBH) bands are used to retrieve the T_{disk} data, which are representative neutral temperatures at an effective height of around 160 km (Evans et al., 2018; Laskar et al., 2021). GOLD scans each full disk in about 30 minutes. The retrieval algorithm is an improvement of the code that was used previously to derive temperature from limb measurements of N_2 LBH intensity from the High-resolution Ionospheric and Thermospheric Spectrograph (HITS) instrument (Aksnes et al., 2006; Krywonos et al., 2012). GOLD measurements have a higher spectral resolution that includes N_2 LBH band emissions within $132 - 162$ nm range. Effective neutral temperatures are retrieved by fitting the observed rotational structure of the N_2 LBH bands using an optimal estimation routine (Rodgers, 2000; Lumpe et al., 2002; Evans et al., 2018). Five parameters are retrieved from each measured spectrum: rotational temperature (K), wavelength shift and dispersion (nm), background (counts/bin), and a forward model scale factor. The current investigation used Level 2 (L2) T_{disk} version 3 data that are retrieved from 2×2 binned level-1C N_2-LBH spectra, which are available at the GOLD web-page, `https://gold.cs.ucf.edu/`. The 2×2 binned data have a spatial resolution of 250-km$\times$250-km near nadir.

3 Results

Sub-satellite local time (Sub-Sat. LT) versus day-to-day variation of GOLD T_{disk} (from here on temperature or in short T) for about 2.5 years (14 October 2018 to 15 March 2021) of observations with ap index and solar F10.7 flux are shown in Figure 1(a). These are averaged between 21°N to 53°N and 43°W to 54°W from the disk observations. This spatial bin is chosen arbitrarily and any other spatial combination also shows similar behavior. But selection of a very narrow bin results in a noisy signal. The average uncertainty, which varies with LBH emission signal-to-noise-ratio, within the above chosen spatial bin is about 12 K. Notable features in this figure are: (a) the temperature is highest near 13-14 LT and afternoon is warmer than morning, and (b) the temperature increases over all local times in response to an increase in ap index or F10.7 flux. Figure

1(b) shows temperature deviations (ΔT) from a baseline local time behavior. The baseline levels are calculated using all the quiet days (with ap<6 nT) that are within a 31 day running window of observation. We choose a 31 day window so that the seasonal changes are also removed once we subtract the 31-day mean. A shorter window will have fewer days with ap<6 nT and also we do not want to remove variations shorter than 30 days, where most of the dominant geomagnetic variations fall.
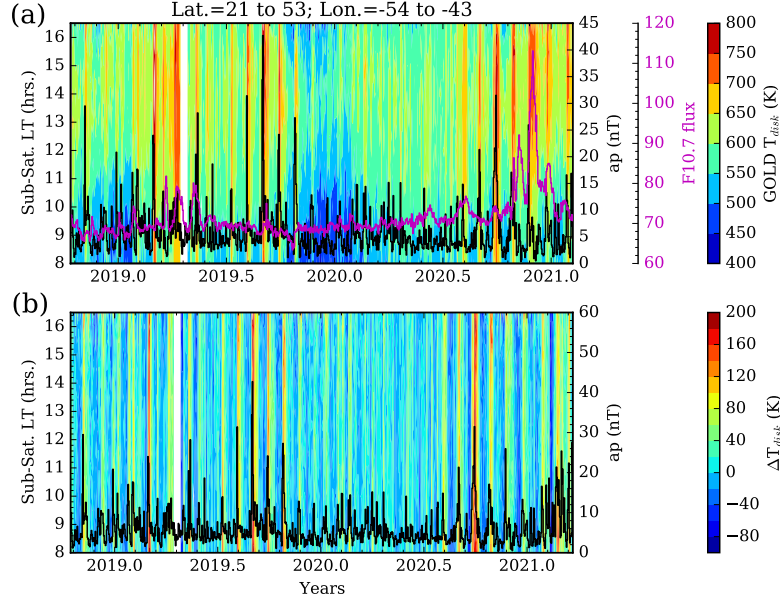
Figure 1. Sub-satellite local time and day-to-day variation of GOLD temperature for about 2.5 years of observations along with ap index and solar F10.7 cm flux are shown in (a). ΔT and ap index variation are shown in (b). Notable feature is the enhancement in T and ΔT as the ap index increase.

Though the solar flux has not exceeded 120 sfu (1 sfu=10^{-22} Wm^{-2}Hz^{-1}) during the period covered in this study, the temperatures show some increase with the slight enhancement in F10.7 cm flux during the last quarter of 2020, where it was above 110 sfu for a couple of days. This temperature increase with F10.7 cm flux is above the mean uncertainty, which is about 12 K. A notable feature of ΔT, as shown in Figure 1(b), is that it increases with increasing ap index. Thus, observations in Figure 1 demonstrate that the GOLD temperature appear to respond to both solar flux and geomagnetic activity. These findings are in consistent with the response observed in GOLD exospheric temperatures due to minor geomagnetic activity reported by Evans et al. (2020). There

161   is a gap of about 10 days of data during 16-26 April 2019, where the GOLD channel-A

162   detector gain was low, which needed a grating yaw maneuver to overcome this. The data

163   during this interval are available but should be interpreted with caution. Thus, they are

164   are not used in the present investigation.

165   To quantify the relationship between ap and ΔT, a scatter plot and a linear regres-

166   sion analysis are shown in Figure 2(a). The scatter plot and the correlation analysis are

167   done with the averaged ΔT values between 21°N to 53°N and 43°W to 54°W and 10 hr

168   to 14 hr local time for all the days with ap>8 nT. Each point in the scatter plot repre-

169   sents a day, as these ΔT values are local-time and spatial averaged as mentioned above.

170   A correlation coefficient of ~0.52 is observed between ap and ΔT, which indicates that

171   they are positively, though weakly, correlated. The not so strong positive correlation be-

172   tween ap and ΔT can be due to other sources of temperature variability, e.g., lower at-

173   mospheric waves (Laskar et al., 2013, 2014) and non-linear response of temperature to

174   geomagnetic-forcing (Connor et al., 2016), and solar flux variability. To further quan-

175   tify their variabilities, Lomb-Scargle periodograms (Horne & Baliunas, 1986) of ap, F10.7,

176   and T_{disk} are shown in Figure 2(b). Almost all the dominant periodicites that are seen

177   in ap, such as, 6, 7, 9, 13-15, and 23-30 days can also be seen in T_{disk}. These results demon-

178   strate that the thermospheric temperature responds positively to geomagnetic activity.

179   The F10.7 cm flux show some dominant periodicities around 27-day, the solar rotational

180   period, which can also be seen in T_{disk} and ap periodicities.

181   As GOLD provides good latitude coverage from 69°S to 69°N, a latitudinal vari-

182   ation of correlation coefficients between ap and ΔT (similar to Figure 2(a)) is shown in

183   Figure 3(a) for two ap ranges, 8-14 nT and $\geq$14 nT. The number of days with 8 nT$\leq$ap<14

184   nT and ap$\geq$14 are 111 and 52, respectively. Some of the active events lasted for more

185   than a day, so the number of individual active periods with 8 nT$\leq$ap<14 nT and ap>14

186   nT were at least 50 and 27, respectively. The latitudinal variation of ΔT for the two ge-

187   omagnetic activity ranges is shown in Figure 3(b). The temperature retrieval algorithm

188   is not optimized to take into account the changes in LBH emissions due to energetic par-

189   ticle precipitation, so latitudes higher than 60° are not considered in this analysis. Note

190   that the correlation coefficients are positive at all latitudes and are higher for stronger

191   geomagnetic events. Also, the temperature enhancements are always positive and are

192   greater at higher mid-latitudes. The greater ΔT enhancements at higher mid-latitudes

193   are in accordance with the fact that most of the energy deposition of the storm time par-
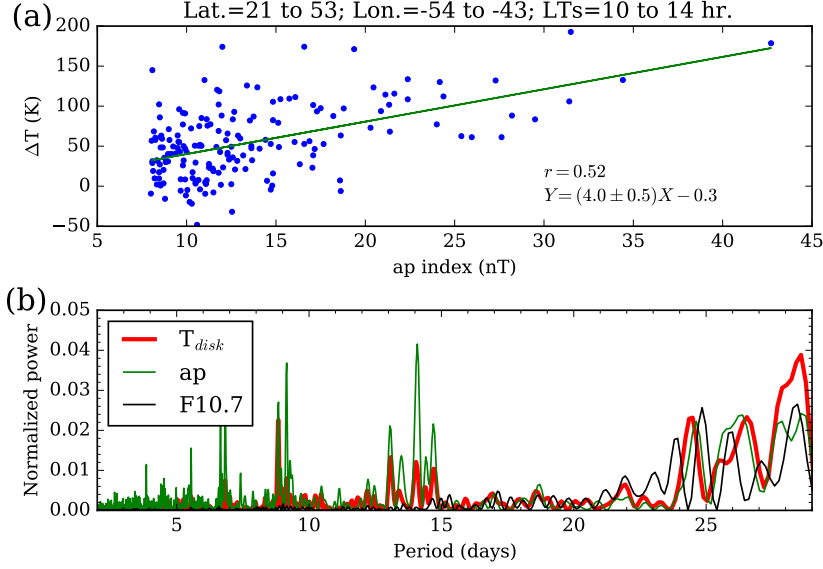
Figure 2. Scatter plot and linear regression with Pearson correlation coefficient between ΔT and ap are shown in (a). Lomb-Scargle periodograms of ap, F10.7, and ΔT are shown in (b). A positive correlation of about 0.52 is observed at latitudes between 21-53°N. Periodogram analysis shows that most of the dominant peaks in ΔT can also be seen in ap.

ticle precipitation occurs at high-latitudes. It also demonstrates that the temperature enhancements occur over all latitudes. The percentage increase in ΔT varies from 10 to 20% for the stronger events. These percentages are for an average of all the 27 individual events having ap≥14 nT. However, the strongest event on 31 August and 1 September 2019 with a daily average ap of 43 nT showed about 25 to 35% enhancement in temperature at low- to mid-latitudes. As the ΔT values are calculated using a reference quiet-day that is obtained from a 30 day running mean around the active day, they should be independent of any artifact that may arise from solar zenith angle and emission angle dependence of T_{disk} (Evans et al., 2018).

A unique feature of the GOLD mission is that it provides an unprecedented local time coverage, in addition to a wide spatial coverage. To investigate the local time variabilities, the ΔT variation at northern mid-latitudes (32°N to 53°N) for the days with ap≥20 nT are shown in Figure 4(a). Note that the number of individual active events with ap>20 nT were 16 in the 2.5 years period. Of the 16 active events, many of them lasted for several days. For this analysis only the first day of the active events are con-
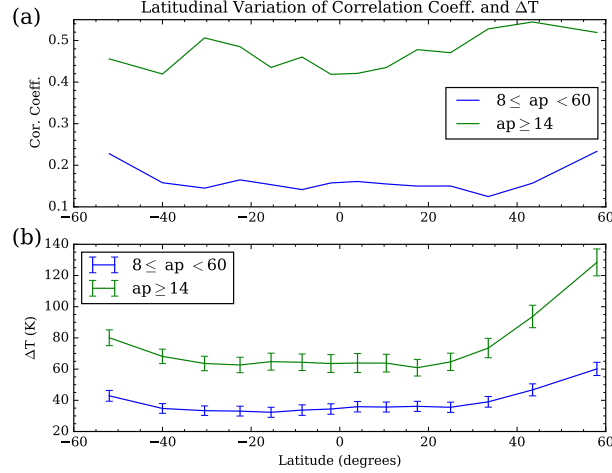
Figure 3. Latitudinal variation of correlation coefficients between ap and ΔT are shown in (a) for two ap limits, 8$\leq$ap<14 nT and ap$\geq$14 nT. Latitudinal variation of ΔT is shown in (b) for the two activity ranges. Correlation coefficients are positive at all latitudes and the temperature enhancements are greater at higher mid-latitudes.

sidered to compare them with a pre-active quiet day. For a particular event, the pre-active quiet day is a day having minimum ap value among 5 consecutive days just prior to the first active day. For most of the events the pre-active quiet day falls 2 to 3 days before the first active day. As there are 16 individual active events having ap>20 nT, the calculations in Figure 4 used 16 active and 16 quiet days. Average ap indices for the 16 quiet and 16 active days were 2.9 nT and 25.4 nT, respectively. Also, the average F10.7 cm flux for the quiet and active days were 72.1 sfu and 73.0 sfu, i.e., they are nearly same. It can be seen that there is more than 90 K difference between active and quiet times at all local times, which cannot be attributed to the 1 sfu increase in F10.7 cm flux. Note that the morning time (8 to 12 LT) temperature deviations are 23.5$\pm$2.5 K larger compared to afternoon time (12.5-16.5 LT). Such morning and afternoon temperature differences occur at all latitudes though the values are lower at low-latitudes (not shown here). This morning and afternoon difference is higher for the stronger events and they are nearly absent, even at mid-latitudes, for events having ap index less than 20 nT. The strongest geomagnetic event during the current observation period is of moderate strength that occurred during 31 August to 1 September 2019. In the future, when we expect a greater number of moderate and severe geomagnetic storms, a quantitative investigation

₂₂₆ of the relationship between strength of geomagnetic activity and corresponding morning to afternoon temperature difference could be performed.
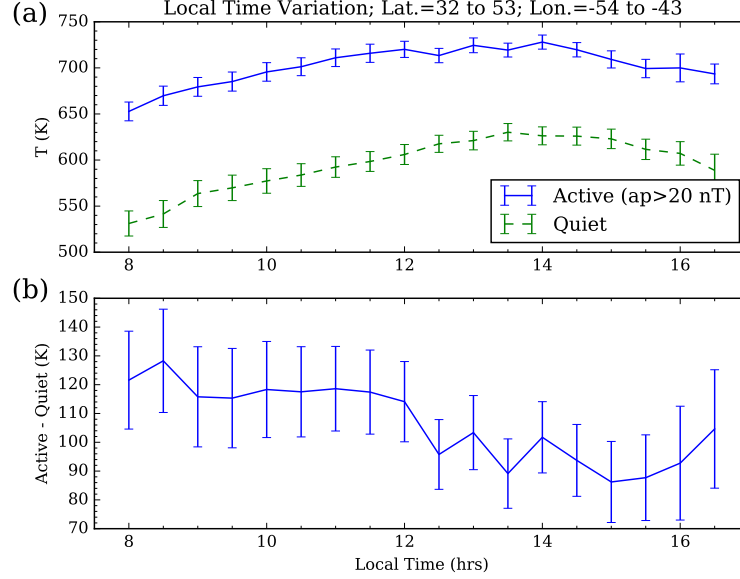
Figure 4. Mean ΔT variations at northern low- to mid-latitudes for all the days with ap>20 nT and average of their corresponding pre-storm (Quiet) days are shown in (a). The difference between active and quiet days are shown in (b). Morning time (8 to 12 LT) differences are greater compared to afternoon time (after 12 LT).

₂₂₇

₂₂₈ 4 Discussion

₂₂₉ Heating due to solar Extreme-Ultra-Violet (EUV) absorption and cooling due to ₂₃₀ downward heat transport is the primary source and sink of energy in the daytime thermosphere. The diurnal tidal circulation in the thermosphere is mainly driven by in-situ ₂₃₂ differential heating due to solar EUV. As a result of this circulation there occur regions ₂₃₃ of convergence and divergence that produce vertical motions (Laskar et al., 2017), which ₂₃₄ are upward in the daytime and are downward in the majority of the night-sector at low- ₂₃₅ and mid-latitudes (Mayr et al., 1978; Burns et al., 1995). From numerical model simulations, Burns et al. (1995) showed that under quiet geomagnetic conditions the usual ₂₃₇ vertical winds during late-night to late-morning are downward and that they are upward ₂₃₈ in the afternoon and late-evening sector. During geomagnetically active events the usual

239 thermospheric equator to pole circulation gets disturbed. Under such altered circulation,

240 the morning time vertical winds at low- and mid-latitudes become more downward due

241 to pole to equator circulation thus creating greater compressional heating compared to

242 quiet time. Whereas, in the afternoon and evening sectors, the storm time circulation

243 makes the vertical winds weaker, resulting in lesser expansion of the thermosphere and

244 thus lesser cooling. Due to this changes in circulation, the storm-time temperatures at

245 low- and mid-latitudes are higher than quiet time. This mechanism also explains why

246 the pre-noon sector enhancement in thermospheric temperature is greater than in the

247 afternoon. Figure 8 of Burns et al. (1995) shows a numerical simulation result that pro-

248 vides a more detailed explanation of this mechanism. The DE-2 data used in Burns et

249 al. (1995) were extremely limited to demonstrate it unambiguously. Our results from the

250 GOLD T_{disk} observations showing morning and afternoon difference as shown in Fig-

251 ure 4, thus provide a first experimental demonstration of this effect during geomagnet-

252 ically active conditions. This also demonstrates that the thermospheric weather plays

253 an important role in responding to geomagnetic forcing effects during active geomagnetic

254 conditions. This has been possible due to the unprecedented local-time and latitude cov-

255 erage of the GOLD mission. In the future, a more detailed investigation of GOLD ob-

256 servations during stronger geomagnetic storms could be performed to quantify the tem-

257 poral relationship between different phases of the storms and ΔT.

5 Conclusions

259 An investigation of the response of thermospheric temperatures to geomagnetically

260 active events of varying magnitudes is carried out using recently available GOLD L2 T_{disk}

261 data. The salient results of this investigation are:

262   1. GOLD T_{disk} measurements respond to geomagnetic activity of varying magnitudes

263   and the response is proportional to the strength of the activity.

264   2. T_{disk} responds to even minor geomagnetic activity with an ap values less than 14

265   nT.

266   3. The temperature enhancement increases with increasing latitude and they are ob-

267   served to vary from 10-35% for weak to moderate events.

268   4. The pre-noon increase in temperature is about 23°K larger than the afternoon one

269   for the active events with ap>20 nT. This demonstrates that the usual daytime

circulation and storm altered circulation work in phase in the pre-noon sector. This also provides a first experimental demonstration of earlier numerical model simulation studies.

These observational results demonstrate, for the first time, the interplay between thermospheric weather and geomagnetic forcing effects during geomagnetically active conditions. This shows that the GOLD T_{disk} data can be used for space weather and operational use. Possible future investigations could be done on the latitude, longitude, and local time dependence of the storms and their spatio-temporal relationship with different phases of the storms.

References

Aksnes, A., Eastes, R., Budzien, S., & Dymond, K. (2006). Neutral temperatures in the lower thermosphere from N_2 Lyman-Birge-Hopfield (LBH) band profiles. *Geophysical Research Letters*, *33*(15). doi: 10.1029/2006gl026255

Aksnes, A., Eastes, R., Budzien, S., & Dymond, K. (2007, June). Dependence of neutral temperatures in the lower thermosphere on geomagnetic activity. *Journal of Geophysical Research: Space Physics*, *112*(A6). doi: 10.1029/2006ja012214

Astafyeva, E., Bagiya, M. S., Förster, M., & Nishitani, N. (2020, March). Unprecedented hemispheric asymmetries during a surprise ionospheric storm: A game of drivers. *Journal of Geophysical Research: Space Physics*, *125*(3). doi: 10.1029/2019ja027261

Bagiya, M. S., Hazarika, R., Laskar, F. I., Sunda, S., Gurubaran, S., Chakrabarty, D., . . . Pallamraju, D.   (2014, July).   Effects of prolonged southward interplanetary magnetic field on low-latitude ionospheric electron density. *Journal of Geophysical Research: Space Physics*, *119*(7), 5764–5776.   doi: 10.1002/2014ja020156

Biondi, M. A., & Meriwether, J. W. (1985, May). Measured response of the equatorial thermospheric temperature to geomagnetic activity and solar flux changes. *Geophysical Research Letters*, *12*(5), 267–270. doi: 10.1029/gl012i005p00267

Burns, A. G., & Killeen, T. L.   (1992, May).   The equatorial neutral thermospheric response to geomagnetic.   *Geophysical Research Letters*, *19*(10), 977–980. doi: 10.1029/92gl00522

Burns, A. G., Killeen, T. L., Deng, W., Carignan, G. R., & Roble, R. G.   (1995). Geomagnetic storm effects in the low- to middle-latitude upper thermosphere. *Journal of Geophysical Research*, *100*(A8), 14673. doi: 10.1029/94ja03232

Cai, X., Burns, A. G., Wang, W., Qian, L., Liu, J., Solomon, S. C., . . . Batista, I. S.   (2021, February).   Observation of postsunset OI 135.6 nm radiance enhancement over south america by the GOLD mission.   *Journal of Geophysical Research: Space Physics*, *126*(2). Retrieved from https://doi.org/10.1029/2020ja028108 doi: 10.1029/2020ja028108

Cai, X., Burns, A. G., Wang, W., Qian, L., Solomon, S. C., Eastes, R. W., . . . McClintock, W. E.   (2020, September).   The two-dimensional evolution of thermospheric $\sum$O/N$_2$ response to weak geomagnetic activity during solar-minimum observed by GOLD.   *Geophysical Research Letters*, *47*(18).   doi: 10.1029/2020gl088838

Chakrabarty, D., Pant, T. K., Sekar, R., Taori, A., Modi, N. K., & Narayanan, R. (2002, February).   Thermospheric temperature and magnetic field measurements from mt abu during a geomagnetically disturbed period – a case study. *Current Science*, *83*(2), 167–170.   Retrieved from www.jstor.org/stable/24106222

Connor, H. K., Zesta, E., Fedrizzi, M., Shi, Y., Raeder, J., Codrescu, M. V., & Fuller-Rowell, T. J.   (2016).   Modeling the ionosphere-thermosphere response to a geomagnetic storm using physics-based magnetospheric energy input: OpenGGCM-CTIM results.   *Journal of Space Weather and Space Climate*, *6*,

A25. doi: 10.1051/swsc/2016019

Crowley, G., Hackert, C. L., Meier, R. R., Strickland, D. J., Paxton, L. J., Pi, X., . . . Wene, G. (2006, October). Global thermosphere-ionosphere response to onset of 20 november 2003 magnetic storm. *Journal of Geophysical Research*, *111*(A10). Retrieved from `https://doi.org/10.1029/2005ja011518` doi: 10.1029/2005ja011518

Deng, W., Killeen, T. L., Burns, A. G., Johnson, R. M., Emery, B. A., Roble, R. G., . . . Gary, J. B. (1995). One-dimensional hybrid satellite track model for the dynamics explorer 2 (DE 2) satellite. *Journal of Geophysical Research*, *100*(A2), 1611. doi: 10.1029/94ja02075

Eastes, R. W., McClintock, W. E., Burns, A. G., Anderson, D. N., Andersson, L., Aryal, S., . . . Woods, T. N. (2020, June). Initial observations by the GOLD mission. *Journal of Geophysical Research: Space Physics*, *125*(7). doi: 10.1029/2020ja027823

Eastes, R. W., Solomon, S. C., Daniell, R. E., Anderson, D. N., Burns, A. G., England, S. L., . . . McClintock, W. E. (2019, August). Global-scale observations of the equatorial ionization anomaly. *Geophysical Research Letters*, *46*(16), 9318–9326. doi: 10.1029/2019gl084199

Evans, J. S., Eastes, R., Lumpe, J. D., Correira, J., Burns, A. G., McClintock, B., . . . Veibell, V. (2018, December). Global-scale Observations of the Limb and Disk (GOLD): Overview of Daytime Neutral Temperature Science Data Product. In *Agu fall meeting abstracts* (Vol. 2018, p. SA21A-3172).

Evans, J. S., Lumpe, J. D., Correira, J., Veibell, V., Kyrwonos, A., McClintock, W. E., . . . Eastes, R. W. (2020, August). Neutral exospheric temperatures from the GOLD mission. *Journal of Geophysical Research: Space Physics*, *125*(9). doi: 10.1029/2020ja027814

Fagundes, P., Sahai, Y., Takahashi, H., Gobbi, D., & Bittencourt, J. (1996, December). Thermospheric and mesospheric temperatures during geomagnetic storms at 23°S. *Journal of Atmospheric and Terrestrial Physics*, *58*(16), 1963–1972. doi: 10.1016/0021-9169(96)00001-3

Forbes, J. M., Gonzalez, R., Marcos, F. A., Revelle, D., & Parish, H. (1996, February). Magnetic storm response of lower thermosphere density. *Journal of Geophysical Research: Space Physics*, *101*(A2), 2313–2319. doi:

10.1029/95ja02721

Fuller-Rowell, T. J., Codrescu, M. V., Moffett, R. J., & Quegan, S. (1994). Response of the thermosphere and ionosphere to geomagnetic storms. *Journal of Geophysical Research*, *99*(A3), 3893. doi: 10.1029/93ja02015

Horne, J. H., & Baliunas, S. L. (1986, March). A prescription for period analysis of unevenly sampled time series. *The Astrophysical Journal*, *302*, 757. doi: 10.1086/164037

Karan, D. K., & Pallamraju, D. (2018, May). Effect of geomagnetic storms on the daytime low-latitude thermospheric wave dynamics. *Journal of Atmospheric and Solar-Terrestrial Physics*, *170*, 35–47. doi: 10.1016/j.jastp.2018.02.003

Killeen, T., Burns, A., Azeem, I., Cochran, S., & Roble, R. (1997, April). A theoretical analysis of the energy budget in the lower thermosphere. *Journal of Atmospheric and Solar-Terrestrial Physics*, *59*(6), 675–689. doi: 10.1016/s1364-6826(96)00114-9

Krywonos, A., Murray, D. J., Eastes, R. W., Aksnes, A., Budzien, S. A., & Daniell, R. E. (2012, September). Remote sensing of neutral temperatures in the Earth's thermosphere using the Lyman-Birge-Hopfield bands of N_2: Comparisons with satellite drag data. *Journal of Geophysical Research: Space Physics*, *117*(A9). doi: 10.1029/2011ja017226

Laskar, F. I., Chau, J. L., St.-Maurice, J. P., Stober, G., Hall, C. M., Tsutsumi, M., ... Hoffmann, P. (2017, September). Experimental evidence of arctic summer mesospheric upwelling and its connection to cold summer mesopause. *Geophysical Research Letters*, *44*(18), 9151–9158. doi: 10.1002/2017gl074759

Laskar, F. I., Eastes, R. W., Martinis, C. R., Daniell, R. E., Pedatella, N. M., Burns, A. G., ... Codrescu, M. V. (2020, July). Early morning equatorial ionization anomaly from GOLD observations. *Journal of Geophysical Research: Space Physics*, *125*(7). doi: 10.1029/2019ja027487

Laskar, F. I., Pallamraju, D., Lakshmi, T. V., Reddy, M. A., Pathan, B. M., & Chakrabarti, S. (2013, July). Investigations on vertical coupling of atmospheric regions using combined multiwavelength optical dayglow, magnetic, and radio measurements. *Journal of Geophysical Research: Space Physics*, *118*(7), 4618–4627. doi: 10.1002/jgra.50426

Laskar, F. I., Pallamraju, D., & Veenadhari, B. (2014, August). Vertical coupling

of atmospheres: dependence on strength of sudden stratospheric warming and solar activity. *Earth, Planets and Space*, *66*(1). doi: 10.1186/1880-5981-66-94

Laskar, F. I., Pedatella, N. M., Codrescu, M. V., Eastes, R. W., Evans, J. S., Burns, A. G., & McClintock, W. (2021, January). Impact of GOLD retrieved thermospheric temperatures on a whole atmosphere data assimilation model. *Journal of Geophysical Research: Space Physics*, *126*(1). doi: 10.1029/2020ja028646

Li, J., Wang, W., Lu, J., Yuan, T., Yue, J., Liu, X., . . . Li, Z. (2018). On the responses of mesosphere and lower thermosphere temperatures to geomagnetic storms at low and middle latitudes. *Geophysical Research Letters*, *45*(19), 10,128-10,137. doi: 10.1029/2018GL078968

Liu, H., & Lühr, H. (2005, August). Strong disturbance of the upper thermospheric density due to magnetic storms: CHAMP observations. *Journal of Geophysical Research: Space Physics*, *110*(A9). Retrieved from https://doi.org/10.1029/2004ja010908 doi: 10.1029/2004ja010908

Liu, X., Yue, J., Wang, W., Xu, J., Zhang, Y., Li, J., . . . Nakamura, T. (2018, May). Responses of lower thermospheric temperature to the 2013 st. patrick's day geomagnetic storm. *Geophysical Research Letters*, *45*(10), 4656–4664. doi: 10.1029/2018gl078039

Lumpe, J. D., Bevilacqua, R. M., Hoppel, K. W., & Randall, C. E. (2002, November). POAM III retrieval algorithm and error analysis. *Journal of Geophysical Research: Atmospheres*, *107*(D21), ACH 5–1–ACH 5–32. Retrieved from https://doi.org/10.1029/2002jd002137 doi: 10.1029/2002jd002137

Mandal, S., & Pallamraju, D. (2020, December). Thermospheric gravity wave characteristics in the daytime over low-latitudes during geomagnetic quiet and disturbed conditions. *Journal of Atmospheric and Solar-Terrestrial Physics*, *211*, 105470. doi: 10.1016/j.jastp.2020.105470

Mayr, H. G., Harris, I., & Spencer, N. W. (1978, November). Some properties of upper atmosphere dynamics. *Reviews of Geophysics*, *16*(4), 539–565. doi: 10.1029/rg016i004p00539

McClintock, W. E., Eastes, R. W., Beland, S., Bryant, K. B., Burns, A. G., Correira, J., . . . Veibel, V. (2020, May). Global-scale observations of the limb and disk mission implementation: 2. observations, data pipeline, and level 1 data products. *Journal of Geophysical Research: Space Physics*, *125*(5). doi:

10.1029/2020ja027809

Mehta, P. M., Walker, A. C., Sutton, E. K., & Godinez, H. C. (2017, April). New density estimates derived using accelerometers on board the CHAMP and GRACE satellites. *Space Weather*, *15*(4), 558–576. doi: 10.1002/ 2016sw001562

Meier, R. R., Picone, J. M., Drob, D., Bishop, J., Emmert, J. T., Lean, J. L., ... Gibson, S. T. (2015, January). Remote sensing of earth's limb by TIMED/GUVI: Retrieval of thermospheric composition and temperature. *Earth and Space Science*, *2*(1), 1–37. doi: 10.1002/2014ea000035

Mikhailov, A. V., & Perrone, L. (2020, January). Poststorm thermospheric NO over-cooling? *Journal of Geophysical Research: Space Physics*, *125*(1). doi: 10 .1029/2019ja027122

Pallamraju, D., Chakrabarti, S., & Valladares, C. E. (2004, September). Magnetic storm-induced enhancement in neutral composition at low latitudes as inferred by O(^{1}D) dayglow measurements from chile. *Annales Geophysicae*, *22*(9), 3241–3250. doi: 10.5194/angeo-22-3241-2004

Pallamraju, D., Laskar, F. I., Singh, R. P., Baumgardner, J., & Chakrabarti, S. (2013, October). MISE: A multiwavelength imaging spectrograph using echelle grating for daytime optical aeronomy investigations. *Journal of Atmospheric and Solar-Terrestrial Physics*, *103*, 176–183. doi: 10.1016/j.jastp.2012.12.003

Pant, T. K., & Sridharan, R. (1998, November). A case-study of the low-latitude thermosphere during geomagnetic storms and its new representation by improved MSIS model. *Annales Geophysicae*, *16*(11), 1513–1518. doi: 10.1007/s00585-998-1513-8

Pant, T. K., & Sridharan, R. (2001, July). Seasonal dependence of the response of the low latitude thermosphere for external forcings. *Journal of Atmospheric and Solar-Terrestrial Physics*, *63*(10), 987–992. doi: 10.1016/s1364-6826(01) 00011-6

Prölss, G. W. (1980). Magnetic storm associated perturbations of the upper at-mosphere: Recent results obtained by satellite-borne gas analyzers. *Reviews of Geophysics*, *18*(1), 183. doi: 10.1029/rg018i001p00183

Rishbeth, H., & Garriott, O. K. (1969). *Introduction to ionospheric physics.* New York: Academic Press.

Rodgers, C. D. (2000). *Inverse methods for atmospheric sounding.* WORLD SCIEN-TIFIC. Retrieved from `https://doi.org/10.1142/3171` doi: 10.1142/3171

Spencer, N. W., Wharton, L. E., Niemann, H. B., Hedin, A. E., Carrignan, G. R., & Maurer, J. C. (1981, December). The Dynamics Explorer Wind and Temperature Spectrometer. *Space Science Instrumentation*, *5*, 417-428.

Strickland, D. J., Cox, R. J., Meier, R. R., & Drob, D. P. (1999, March). Global o/n2derived from DE 1 FUV dayglow data: Technique and examples from two storm periods. *Journal of Geophysical Research: Space Physics*, *104*(A3), 4251–4266. Retrieved from `https://doi.org/10.1029/98ja02817` doi: 10.1029/98ja02817

Tsurutani, B. T., Verkhoglyadova, O. P., Mannucci, A. J., Saito, A., Araki, T., Yumoto, K., . . . Vasyliūnas, V. M. (2008, May). Prompt penetration electric fields (PPEFs) and their ionospheric effects during the great magnetic storm of 30-31 october 2003. *Journal of Geophysical Research: Space Physics*, *113*(A5), n/a–n/a. doi: 10.1029/2007ja012879

Zhang, Y., Paxton, L. J., & Schaefer, R. K. (2019, July). Deriving thermospheric temperature from observations by the global ultraviolet imager on the thermosphere ionosphere mesosphere energetics and dynamics satellite. *Journal of Geophysical Research: Space Physics*, *124*(7), 5848–5856. doi: 10.1029/2018ja026379